The Role of Bi^{3+}-complex Ion as the Stabilizer in Electroless Nickel Plating Process

K. Wang
Dept. of Chemical and Biomolecular Engineering, National University of Singapore, BLK E5 02-02, 4 Engineering Drive 4, Singapore 117576

L. Hong
Dept. of Chemical and Biomolecular Engineering, National University of Singapore, BLK E5 02-02, 4 Engineering Drive 4, Singapore 117576, and Institute of Materials Research & Engineering, 3 Research Link, Singapore 117602

Z-L. Liu
Institute of Materials Research & Engineering, 3 Research Link, Singapore 117602

DOI 10.1002/aic.11807
Published online March 11, 2009 in Wiley InterScience (www.interscience.wiley.com).

Bi^{3+}-complex ion is presented here as a less toxic stabilizer for use in electroless nickel plating (ENP) to replace the existing Pb^{2+} ion stabilizer. The asymmetric derivatives of EDTA are identified to be a type of coordination ligands that can combine with Bi^{3+} ions to form soluble complexes in the acidic ENP solution. In the ENP system studied the Bi^{3+}-complex ion displays a critical stabilizer concentration of about 10^{-5} mol/L, that is, the percolation concentration over which the ENP rate drops sharply. Besides the experimental measurement, deposition rates of both Ni and P are also simulated by using a kinetic model that has been derived from the double electric layer theory. The Bi^{3+}-complex ion, behaving like conventional Pb^{2+} ion, stabilizes ENP bath through the chemical replacement reaction at the surface of Ni deposition layer and results in a passive plating surface. This investigation also verifies the properties of the EN deposit, which are insignificantly affected by the length of service time of the plating solution by employing Bi^{3+}-complex ion stabilizer. *AIChE J,* 55: 1046–1055, 2009
Keywords: electroless nickel plating, Bi^{3+}-complex ion, stabilizer, stabilization mechanism, chemical replacement reaction

Introduction

Electroless nickel plating (ENP) is an important technology aiming for the implementation of a Ni-P alloy thin layer with specific traits like hardness, finished surface, wear and abrasion resistance, and corrosion resistance etc. on the surface of the preferred articles.[1–3] ENP is in nature an autocatalytic process because the disproportionation reaction of hypophosphite ion ($H_2PO_2^-$), and the reduction of Ni^{2+} ions take place on the freshly deposited nickel layer.[3,4] This autocatalytic nature leads to an inherent instability of ENP system due to the production of insoluble colloidal particles of nickel and nickel phosphite in the bulk of plating solution as the metal deposition proceeds. These tiny particles carry a large number of highly reactive catalytic sites due to their tremendous specific surface areas. Consequently, an overwhelming deposition of nickel black is triggered out via a "self-accelerating reaction" or the plating-out process, which indicates the failure of a plating bath.[1–3] Therefore, it is crucial to include a pertinent stabilizer in the ENP system.

Correspondence concerning this article should be addressed to L. Hong at chehongl@nus.edu.sg.

ENP stabilizer is a unique type of reactive species since a trace amount is normally required in the ENP bath to inhibit deposition of nickel black. With such stabilizer, a sufficiently long bath service life can be obtained for industrial applications.[1–3] Although a few ppm of Pb^{2+} is generally present in a commercial ENP bath, with the greater awareness of the hazardous effects of lead in recent years,[5] the use of lead-containing products is strictly barred.[6] Therefore, using lead-free ENP baths has become obligatory. A number of sulfur-containing chemicals, such as thiourea in particular, were proposed to replace lead as the stabilizer in ENP solution. However, the participation of sulfur species in the ENP layer has been a concern for its deteriorative effect on the corrosion resistance of ENP deposits.[7–12]

Among heavy metals, bismuth is unique due to its much lower toxicity than that of its neighbors in the periodic table such as lead, thallium, and antimony. In fact, bismuth has been widely used as a lead substitute in industries,[13,14] because the toxicity of bismuth and its salts is dose-dependent and only large doses can be fatal.[15–17] Furthermore, the existence of insignificant amounts of bismuth in the ENP deposit surface does not undermine its corrosion resistance. Alfons et al.[18] and Bobrovskays et al.[19] reported their studies on replacing lead by bismuth (III). Nevertheless, their studies did not disclose the method of how Bi^{3+} ion was incorporated into weak acidic ENP solution. This is an important issue because Bi^{3+} ion undergoes quick hydrolysis to form white precipitate in ENP solution if there is not a relevant ligand to protect the Bi^{3+} ion. The other problem to look at is the ligand effect on the reactivity of Bi^{3+} ion. Hence, it is meaningful to gain an insight into the coordination chemistry of Bi^{3+} ion in ENP system.

In this work, the three derivatives of EDTA (ethylenediamine tetraacetic acid) (Figure 1) have been found to be able to assist the dissolution of Bi^{3+} ions in the weak acidic ENP solution medium, whereas as a typical chelating complexing agent EDTA itself does not work to serve this aim. Moreover, this work also found that finite structural differences of these ligands do not affect the performance of ENP, such as plating rate, composition of deposition layer, surface morphology and bath service life etc. Hence, this article focuses on the understanding of how the Bi^{3+}-complex ions affect the ENP rate, and the surface properties of Ni-P deposition layer instead of insignificant impacts caused by the structural difference of the three ligands. In addition, a simple theoretical model that uses the same concept as developed in our prior work[20] is proposed to investigate the stabilization mechanism of Bi^{3+} ion in the ENP system, and predict the deposition rates of nickel (R_{Ni}) and phosphorus (R_P), respectively. According to this model, once the Bi^{3+}-complex ions exceeds its critical concentration, an exponential reduction in both nickel and phosphorus deposition rates occurs concurrently. The last part of this article reports the assessment of bath service life. The Bi^{3+}-complex ion stabilizer could sustain a continuous plating process of four metal-turn-overs (MTOs) with a very similar plating rate and the surface properties of Ni-P deposit.

Experimental

Materials

All chemicals used are analytical-grade. Nickel sulfate hexahydrate, sodium hypophosphite monohydrate, ammonium hydroxide and sodium acetate (from Merck) lactic acid and acetone (Fisher Chemical), DL-malic acid (Acros), and bismuth (III) nitrate pentahydrate (Aldrich) were used as received. The brass hull cell test panels (Hiap Guan Electroplating Material Singapore) were used as plating substrate. The prior plating cleaning include degreasing in an alkaline detergent solution for 5 min, with the assistance of ultrasonication and then DI water rinsing.

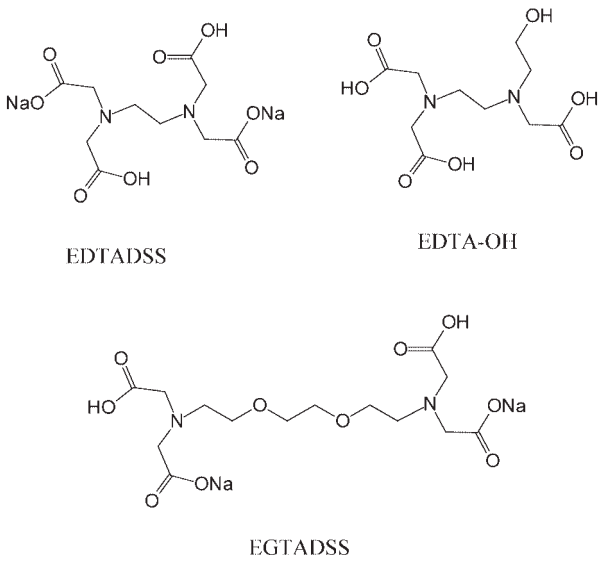

Figure 1. The molecular structure of the three EDTA-derivative ligands.

Effects of stabilizer concentration on ENP rate

The plating solution was formulated and its main components are listed in Table 1. The plating was initiated by touching the substrate with a nickel coil. In this investigation, each data point of a curve was collated from a small plating bath containing plating solution 80 mL, of which pH was adjusted to 5.00 ± 0.05 by the addition of ammonium hydroxide solution (25%) before plating. The temperature of plating solution was maintained at 90°C by using water bath (HAAKE DC30/W13) as heating source. The weight of Ni-P layer gained (W) on the brass substrate ($0.25 \times 50 \times 37$ mm^3) after plating for 30 min, was determined by the gravimetric method using an analytical balance (AND GR-200). The deposition rate (r) was computed using the following formula

$$r = \frac{W \times 10^4}{\rho A t}, \tag{1}$$

where r is the deposition rate in μm/h, W the weight of plating layer in gram, A the plating area in cm^2; t the plating time in hours, and $\rho = 7.8 g/cm^2$ is taken as the density of Ni-P alloy by assuming $P \cong 13\%$.

Electrochemical analysis of the oxidation rate of hypophosphite

The anodic reaction of hypophosphite in the presence of Bi^{3+} complex ion was evaluated by the linear-sweep

Table 1. Composition of ENP solution

Components	Concentration
Nickel (II) sulfate hexahydrate	22.4 g/L
Sodium hypophosphite monohydrate	25 g/L
DL-Malic Acid	4 g/L
Sodium Acetate	8.5 g/L
Lactic Acid	21 ml/L
Stabilizers	variable

*The molar ratio of complexing agent to Bi^{3+} was maintained at 2:1 for the three Bi-complex stabilizers.

voltammetry (Autolab, Model JP202). The experiment was carried out in an electrochemical cell equipped with three-electrodes (CFC-13 Coating Flat Cell, Scrinberassociate, USA). The working electrode was a piece of plated brass plate (13 cm^2), the counter-electrode was an platinum-mesh with a surface area of 25 cm^2, and the reference electrode was a standard Ag/AgCl electrode (Metrohm 6.0726.100, Switzerland). The solution used contained sodium hypophosphite and a Bi^{3+}-complex stabilizer whose concentration was varied, and the pH value of solution was maintained at 5.00 $\pm$ 0.03. This solution was kept still and maintained at 70°C during potential scanning unless otherwise noted. The current-potential curves were obtained from a potential scan with a rate of 10 mV/s.

Assessment of ENP bath stability

The initial conditions of both plating bath and the substrate were the same as those described in the Effects of stabilizer concentration on ENP rate section. As the electroless plating proceeds, the pH of plating bath was maintained at 5.00 $\pm$ 0.05 by frequent addition of 25% ammonium hydroxide solution. The plating solution was agitated using mild air bubbling throughout the entire process. The stabilizer concentration in this metal-turn-over (MTO) testing process was kept around 2×10^{-6} M. The plating solution (1.2 L), and the plating load (defined as the plated area in dm^2 divided by the volume of plating solution in L) of 2.5 dm^2/L were fixed throughout the MTO durability test. The plating bath was replenished after each 30-min interval using a concentrated plating solution ($\sim$ 40 mL for each). The stabilizer in the plating bath was replenished at the beginning of each MTO, and the brass substrate was changed after each MTO cycle.

Evaluation of corrosion resistance

The corrosion resistance of the plating layer generated from the each MTO was assessed by potentiodynamic polarization technique. The measurement was conducted in the three-electrode electrochemical system as described in the section entitled *Electrochemical analysis of the oxidation rate of hypophosphite*, using a HCl solution (1M, 100 mL) as the medium. The scanning rate was set at 1 mV/s.

Instrumental analyses

The surface morphology of Ni-P plating layer was studied on a scanning electron microscope of field-emitting (FE-SEM; instrument JEOL, JSM-6700F, Japan). Energy dispersive X-ray spectrometry (EDX; IncaEnergy 400, Oxford Instrument, Ltd.), and X-ray photoelectron spectrometer (XPS; Kratos xis HiS System, using C1s at 284.8eV as reference), were employed to analyze the chemical composition of the Ni-P deposits.

Palladium titration

The effectiveness of Bi^{3+} complex stabilizer was evaluated by palladium titration method as described previously.[21] The aqueous $PdCl_2$ solution was prepared by dissolving $PdCl_2$ of 25mg in 5-mL concentrated hydrochloric acid (37%). The resulting solution was then diluted by DI water to 500 mL in a volumetric flask. Before the titration, the pH of the plating bath was set at 4.80 $\pm$ 0.03 by adding in ammonium hydroxide solution. The $PdCl_2$ solution was dripped at a rate of about 0.05 mL/s into 20 mL ENP solution, keeping the temperature at 60 $\pm$ 2°C. Sufficient magnetic stirring was upheld to disperse the $PdCl_2$ that is added instantaneously. The titration was stopped at the moment when the ENP bath turned black, which is an indication of large precipitation of metal colloids; and the $PdCl_2$ solution consumed was recorded as the decomposition volume V_d. For each concentration, the titration was repeated for 20 times to reduce experimental error. In addition, a parallel study of the effectiveness of Pb^{2+} ion in the same plating system was also evaluated as benchmark.

Results and Discussion

Influence of Bi^{3+}-complex ion on anodic reaction of hypophosphite

Bi^{3+} ion can only exist in fairly strong acidic solutions, because it undergoes rapid hydrolysis in water to generate bismuth oxide (BiO^+), which precipitates as BiO·OH. Hence, it is important to identify a suitable ligand that is able to form complex with Bi^{3+} ion in the weak acidic ENP medium to ensure complete dissolution of the required amount of bismuth salt. With this aim in mind, EDTA derivatives with four nonequivalent chelating arms of ethylenediamine (as shown in Figure 1) were found to be able to form water-soluble complex with Bi^{3+} ion satisfactorily. However, EDTA itself causes precipitation in ENP solution instead. This phenomenon implies that the free arms, other than those that form coordination bond to Bi^{3+} ion, must be reserved in the complex in order to maintain the solubility of complex. We further examined the three complexes using UV–Vis spectroscopy, and found that all of them showed an extremely strong absorption band near 270 nm in contrast with the pristine ligands, which revealed only a weak peak tail in the range of $\lambda > 200$ nm. The same investigation also showed that Ni^{2+} ion cannot replace Bi^{3+} ion in the three types of complexes. The hydrated Ni^{2+} complex shows the maximum absorption at 400 nm, but this wavelength does not shift or become weaker when one of the Bi^{3+}-complexes with equal molar ratio to Ni^{2+} is introduced. Hence, Bi^{3+} ion in the complex is unlikely to be substituted by Ni^{2+} ion in the ENP bath, namely, the three ligands possess much stronger affinity with Bi^{3+} than with Ni^{2+} in aqueous medium.

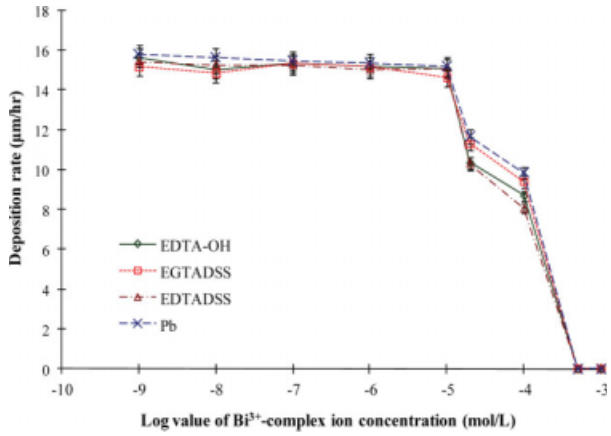

Figure 2. The influence of the concentrations of the Bi^{3+}-complex ions, as well as Pb^{2+} ion on nickel deposition rate.

[Color figure can be viewed in the online issue, which is available at www.interscience.wiley.com.]

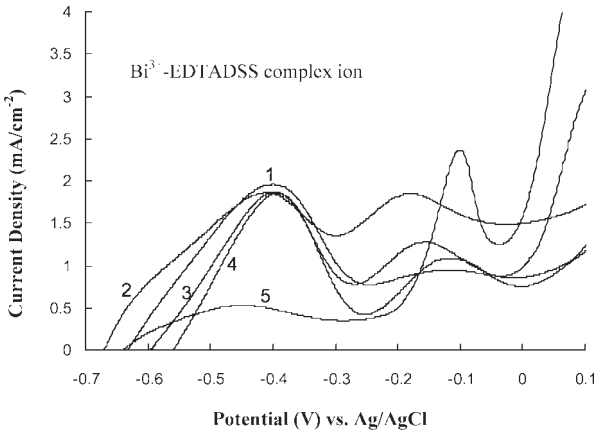

Figure 3. The current density - potential curves of the oxidation of hypophosphite on Ni-P electrode in the solution containing 0.24 mol/L hypophosphite, and the different concentrations of Bi^{3+}-EDTADSS complex: (1) 0 mol/L, (2) 10^{-8} mol/L, (3) 10^{-6} mol/L, (4) 10^{-5} mol/L, and (5) 10^{-4} mol/L.

The charts of ENP rate vs. the concentration of Bi^{3+}-complex ion are shown in Figure 2. All of them reveal a critical concentration at about 10^{-5} mol/L ($C_{Bi\text{-}C}$), over which the deposition rate is decelerated rapidly. In the concentration range from 10^{-9} mol/L to 10^{-5} mol/L, the Bi^{3+}-complex ion does not noticeably influence the nickel deposition rate. In addition, structural differences of the three EDTA-derived ligands do not affect ENP deposition rate in the concentration range below $C_{Bi\text{-}C}$. Hence, the three ligands used in this work are indistinguishable in terms of their effect on ENP process. The rate-concentration curve obtained from employing Pb^{2+} ion stabilizer is included as the reference. ENP can be, in principle, split into the cathodic reaction (Ni-P deposition), and the anodic reaction $H_2PO_2^- + H_2O \rightarrow H_2PO_3^- + 2H^+ + 2e^-$. The anodic half reaction is deemed to be the rate determining step of the whole ENP.[22–25] Hence, the Bi^{3+}-complex ion is expected to retard the anodic reaction when its concentration is above $C_{Bi\text{-}C}$. To verify this concept, the anodic potentiodynamic scanning test was carried out, in which the anodic current density of the working electrode (i.e., a Ni-P layer on brass) generated from the oxidation of hypophosphite anion on the electrode was recorded when the working electrode is given a series of lower biases relative to the reference electrode (Ag/AgCl).

It was observed that all the anodic polarization curves (Figure 3) consist of two peaks, of which the first peak (ca. −0.41V vs. Ag/AgCl) reflects oxidation of hypophosphite ion, and the second one (ca. −0.14V) the dissolving of Ni-P layer.[23–28] As plating rate of cathodic reaction is governed by the anodic current density or the supply of electrons from anodic reaction, the peak intensity that reflects the oxidation rate of hypophosphite ion could, therefore, be taken as a measure of ENP rate at a particular concentration of stabilizer. Hence, with respect to a stabilizer, a plot of anodic current density values (amplitude of peak) vs. concentrations of stabilizer was plotted (Figure 4). Indeed, the current density ~log C relationship is analogous to the deposition rate ~log C relationship as presented in Figure 2. This resemblance verifies the relation that the oxidation of hypophosphite determines the ENP rate. Since the three types of Bi^{3+}-complex ions display similar effect on the rates of both anode and cathode reactions, one of them, EDTADSS-Bi^{3+} complex, was selected to assess the concentration effect of stabilizer on the surface composition of Ni-P plating layer, the agreement between experimental and theoretical deposition rates, and the stabilizing capacity in the following paragraphs.

Similar to what Pb^{2+} ions act in inhibiting the anodic process of ENP, when the concentration of stabilizer is below its critical level ($C_{Bi\text{-}C}$), a handful amount of the surface Ni atoms will be replaced by Bi^{3+} ions through the chemical displacement reaction $Bi^{3+} + \frac{3}{2}Ni \rightarrow Bi + \frac{3}{2}Ni^{2+}$, that is thermodynamically spontaneous ($\Delta G^o \cong -82.5kj \cdot mol^{-1}$). The Bi atoms generated occupy the surface lattice sites of Ni atoms due to their close atomic radii ($r_{Ni} = 124$ pm vs.

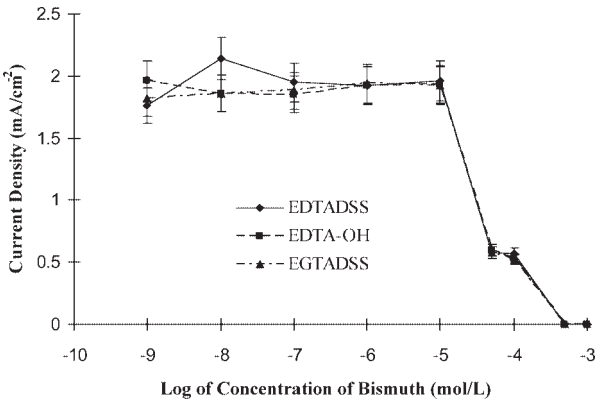

Figure 4. The plots of peak values of anodic current density vs. the corresponding concentrations of Bi^{3+}-complex ions.

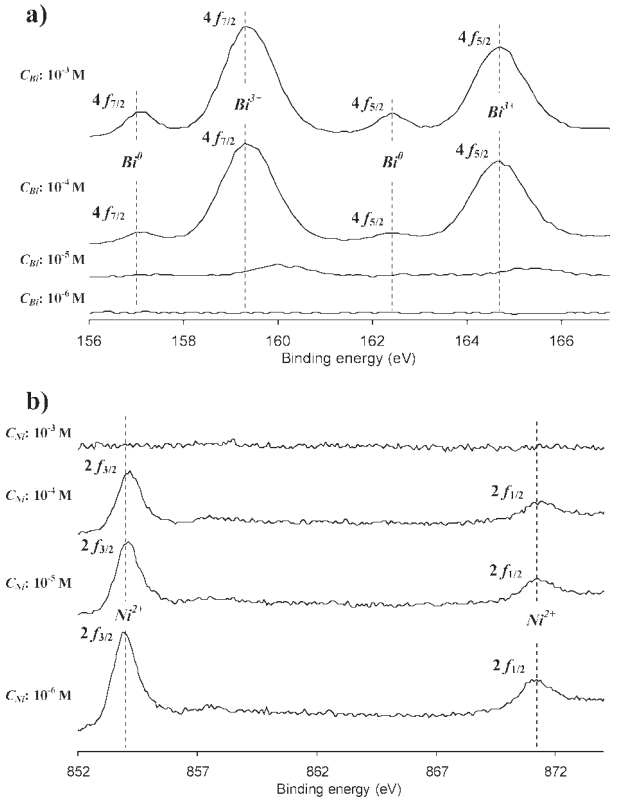

Figure 5. The XPS spectra of (a) Bi 4f and (b) Ni 2p in the four samples after they were plated in ENP bath with using different concentrations of Bi^{3+}- EDTADSS complex ion for 30 min.

$r_{Bi} = 150$ pm). A sparse number of Bi atoms distributed over the surface Ni lattice could be sufficient to make the substrate passive to ENP according to the theoretical model developed previously.[20] It is, however, difficult to detect the presence of Bi at the deposit surface by XPS, due to their substantially low contents (Figure 5a). The two spectra corresponding to the initial stabilizer concentrations (C_{Bi}) of 10^{-5} and 10^{-6} M, respectively, find no traces of Bi species. In order to verify this chemical displacement process, a higher concentration of Bi^{3+}-complex ion (10^{-4} M or 10^{-3} M) relative to $C_{Bi\text{-}C}$ was tested in the same plating system as that designed for generating plots of Figure 2. Although no perceptible Ni deposition (i.e., generation of small H_2 bubbles) on brass substrate took place, since the stabilizer concentration is above $C_{Bi\text{-}C}$, Bi species were still detected on these two samples as manifested by Bi 4*f* doublet peaks on the XPS spectra (Figure 5a). Correspondingly, the XPS Ni 2*p* doublet peaks do not appear on the spectrum of the sample with using the stabilizer concentration of 10^{-3} M (Figure 5b). It is logical to believe that a thin layer of Ni was deposited on a brass plate at the very moment when ENP was initiated by touching the plate with a Ni wire, but the Ni deposit was replaced immediately by Bi through the chemical displacement reaction. Meanwhile, it may be worthy to note that under the same conditions Bi^{3+}-complex ions are not reduced by hypophosphite. As such, the deposition of Bi species on the brass substrates was solely due to the chemical displacement reaction with Ni atoms. A further confirmation was undertaken by EDX analysis (Figure 6). In this experiment a pure Ni-P alloy layer (sample a), which was prepared in the ENP solutions without using a stabilizer, was plated once more but in the ENP solution containing EDTADSS-Bi^{3+} of 10^{-3} M for 30 min. The treated surface layer (sample b) manifested a higher concentration of Bi than Ni and, in addition, a rather thin depth left because the brass was also detected by EDX. This outcome indicates that the initial Ni-P layer was dissolved during the second plating because of the displacement reaction as stated earlier. Furthermore, when inspecting the XPS binding energy of Bi4*f* peaks, two sets of Bi 4*f* doublets consisting of the Bi $4f_{7/2}$ peak and the Bi $4f_{5/2}$ peak, where both peaks are separated by about 5.3–5.6 eV, are observed. Bi $4f_{7/2}$ peak at 159.3 eV, and Bi $4f_{5/2}$ peak at 164.6 eV indicate the presence of Bi^{3+} cations,[29] while Bi(0) is reflected by the two peaks that appear at 156.9 eV and 162.5 eV, respectively.[30] In comparison with the surface concentration of Bi(0) species, a much higher surface concentration of Bi^{3+} species is present, and this could be attributed to fast oxidation of Bi(0) during the washing of the sample before analysis to remove residues of the solution.

Attempts were made to use the theoretical model[20] that was developed previously to simulate the effect of the stabilizer concentration (C_s) on the deposition rates of nickel (R_{Ni}) and phosphorus (R_P). According to this model a

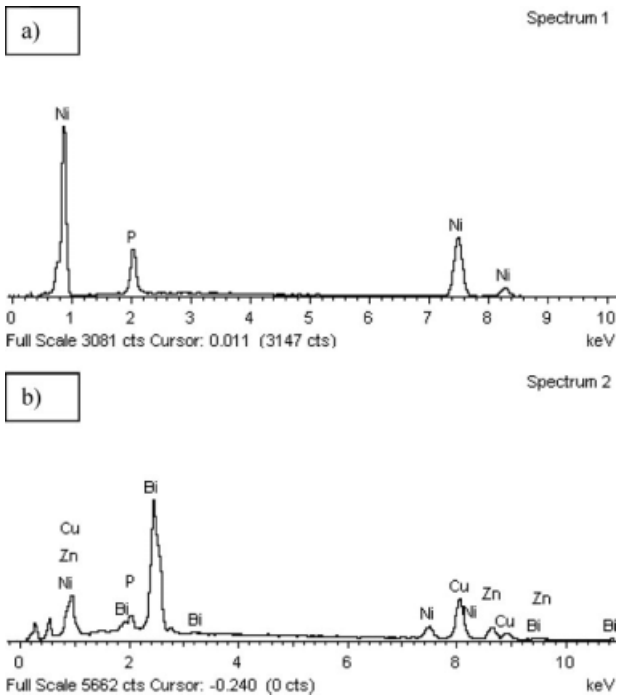

Figure 6. EDX spectra of the two samples: (a) the pristine Ni-P layer obtained from plating a brass plate for 30 min in the ENP solution (Table 1) without using a stabilizer, and (b) the treated Ni-P layer obtained from plating the pristine Ni-P layer for 30 min in the ENP solution containing EDTADSS- Bi^{3+} of 5×10^{-3} mol/L.

mathematical expression of the nickel deposition rate is created by envisioning the electrical double layer (EDL) attached to the surface of substrate as a one-dimensional (1-D) potential well, and the electron transfer from the Fermi level of the substrate to Ni^{2+} ions at the external side of EDL as the quantum tunneling effect. Establishing the relationship between Bi^{3+}-ion concentration and the Fermi level is an important step for deriving the nickel and element phosphorus deposition rates. The stabilizing effect of the bismuth ion is attributed to its participation as the neutral atom in the lattice of the Ni-P layer, which results in the ascension of Fermi level and shifts the electrode potential of Ni-P layer to the negative value direction. Thus, the oxidation of hypophosphite (anodic reaction) at the plating surface is retarded, and it in turn slows down the deposition of both Ni and P that needs electrons. The theoretical deposition rates are represented by the following two equations

$$R_{Ni} = R_{Ni}^0 \sqrt{\frac{E_f^0 + 4\pi pa\left(C_S - C_S^c\right)}{E_f^0}} \times \exp\left[\left(64\pi pa - \frac{4\pi pak_G}{kT}\right)\left(C_S - C_S^c\right)\right] \quad (1)$$

$$R_P = R_P^0 \exp\left[-\frac{4\pi pak_G}{kT}\left(C_S - C_S^c\right)\right] \quad (2)$$

where p is the dipole moment, a is a constant, E_{f0} is the Fermi energy level without the stabilizer, k_G is the $H_2PO_2^-$ adsorption constant, k is the Boltzmann constant, R_{NI}^0 is the nickel deposition rate without stabilizer, R_P^0 is the phosphorus deposition rate without stabilizer, C_S is the stabilizer concentration, and C_S^c the critical stabilizer concentration.

If $4\pi pa\left(C_S - C_S^c\right) \ll E_f^0$, Eq. 1 is then simplified to

$$R_{Ni} = R_{Ni}^0 \exp\left[\left(64\pi pa - \frac{4\pi pak_G}{kT}\right)\left(C_S - C_S^c\right)\right] \quad (3)$$

Then we can simplify Eqs. 2 and 3 as

$$R_{Ni} = K_1 \exp\left(K_2\left(C_S - C_S^c\right)\right) \quad (4a)$$

$$R_P = L_1 \exp\left(L_2\left(C_S - C_S^c\right)\right) \quad (5a)$$

In Eqs. 4a and 5a, there are four physical terms K_1, K_2, L_1 and L_2, whose values are to be determined. This is realized through simulation of these two theoretical models by using the experimental data as shown in Figure 7. Substitution of the parameters obtained from simulation into Eqs. 4a and 5a, the nickel deposition rate R_{Ni}, and the phosphorus deposition rate R_P, in mg/cm2 h, are established as follows

$$R_{Ni} = 11.679 \exp\left(-10837\left(C_S - C_S^c\right)\right) \quad (4b)$$

$$R_P = 1.6449 \exp\left(-7060.9\left(C_S - C_S^c\right)\right) \quad (5b)$$

From the earlier theoretical models, how the Bi^{3+}-complex ion exerts its leverage on the deposition rates of Ni and P, is, therefore, quantified.

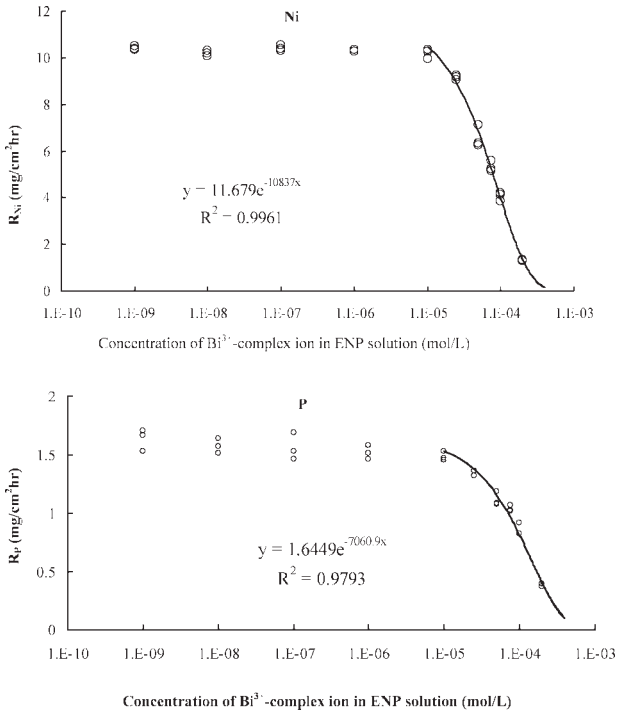

Figure 7. The influence of the Bi^{3+}- EGTADSS ion concentration on the deposition rate of nickel and phosphorus (where open circles represent experimental values and the curves from the theoretical models).

The critical role of metal colloidal particles generated in ENP solution

There is always a trace amount of Ni(0) clusters detaching from the plating frontier, and entering into the solution during the ENP process. These colloidal particles are deactivated due to the chemical displacement of Bi^{3+} on their surface. To verify the presence of metal colloidal particles, a few drops of solution were collected from an ENP bath containing Bi^{3+}-complex ions of 10^{-5} M after plating for 1h, and the liquid sample was dried gradually on a copper grid. It was then observed using TEM (Figure 8). The EDX analysis showed that these colloidal particles are enriched with primarily nickel and bismuth in contrast to the background. No such tiny particles were observed when the fresh solution was sampled.

Palladium titration is another method to test the stabilizing capacity of an ENP bath. Metal nuclei were generated instantaneously when the $PdCl_2$ solution was dropped into the bath, but the bath still remained clear until an adequate volume of $PdCl_2$ solution (V_d) was introduced, in which a black cloud was observed instantly. Unlike Ni^{2+} ion, Pd^{2+} ion could be reduced by hypophosphite ion around 40°C. On the Pd particles generated, a quick Ni deposition takes place and initiates an overwhelming metal powder deposition. Before the bath decomposition is triggered out, the metal colloidal particles (Ni/Pd) are turned passive due to the occupation of Bi on surface sites of these miniature particles.

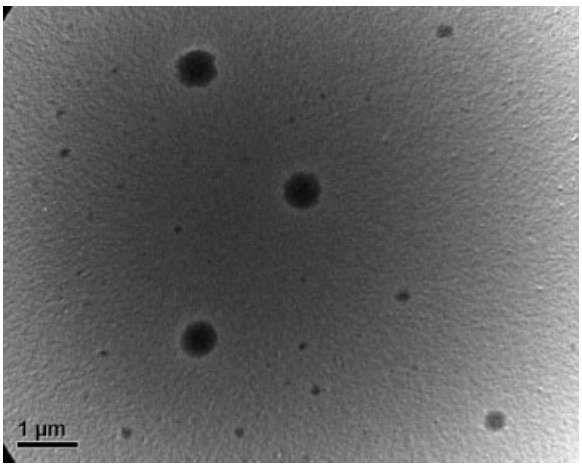

Figure 8. The TEM image of Ni colloidal particles collected from the plating bath where Bi^{3+}-EDTADSS stabilizer (10^{-5} mol/L) was used and had a plating history of 1 h.

It is interesting to note that V_d undergoes almost a negligible increase, with an increase in the concentration of stabilizers in the concentration range below $C_{Bi\text{-}C}$, and a steep increase when its concentration exceeds this critical point (Figure 9). The appearance of such a plateau followed by a hill implies that deactivation of metal colloidal particles requires a substantially low concentration of stabilizer (e.g., 10^{-8} M). In other words, a metal particle become passive when a small number of its surface sites is occupied due to the lift of its Fermi level.[20] The additional stabilizer increases only the surface coverage of existing particles (corresponding to magnitude of V_d), and the turning point in between (10^{-5} and 10^{-4} M) marks the attainment of saturation coverage. After this margin an extra amount of stabilizer will be sufficient to tackle a huge number of newly generated metal particles. This test also reveals that Bi^{3+}-complex ion has a slightly better stabilizing effect than Pb^{2+} ion.

The effect of stabilizer concentration on the performance of ENP bath

It is imperative to understand how the composition of nickel plating layer is affected with the variation of Bi^{3+}-complex ion concentration. Table 2 lists EDX measurement data of Ni wt % and P wt % of the plating layers obtained from different plating bath conditions. The Ni/P atomic ratio in the plating layer maintained approximately 3.5 regardless of the kind of EDTA-derived ligand that was used to form Bi^{3+}-complex ion.

Table 2. The Composition of Ni-P Alloy Deposit Layer Based on EDX Analysis

Concentration of Bi^{3+} ion (mol/L)	EDTADSS		EDTA-OH		EGTADSS	
	Ni %	P %	Ni %	P %	Ni %	P %
0	86.3	13.7	86.3	13.7	86.3	13.7
10^{-9}	86.0	14.0	87.1	12.9	86.2	13.8
10^{-8}	86.7	13.3	87.0	13.0	86.2	13.8
10^{-7}	85.9	14.1	87.8	12.2	87.2	12.8
10^{-6}	86.7	13.3	87.2	12.8	87.5	12.5
10^{-5}	87.0	13.0	87.1	12.9	87.7	12.3

To examine the long-term stabilizing effect of Bi^{3+}-complex ion in ENP bath, a 4-MTO continuous plating process was carried out. It may be noted that the ENP cannot complete even one MTO without the Bi^{3+}-complex due to the reason as in the aforementioned, e.g., in the first paragraph of the Introduction. None of plating-out in the plating bath after 4-MTO was observed despite a very slight decrease in plating rate (Figure 10). In general, although the kind of ligand did not show effect on producing significant discrepancies in the deposition rates, there were still perceptible differences in the rates of 4th-MTO. As the reference, the use of Pb^{2+} ion as the stabilizer leads to a slightly higher plating rate, especially in the first two MTOs, which is consistent with Figure 2. The P% in the plating layer could be maintained roughly stable throughout the four MTOs (Table 3), where the P% in the Ni/P plating layer in all samples is above 10 wt %. This is regarded as the high phosphorus EN deposition that is generally considered to possess good corrosion resistance.[31,32] To verify this feature, the potentiodynamic scanning (PDS) technique (see the section entitled

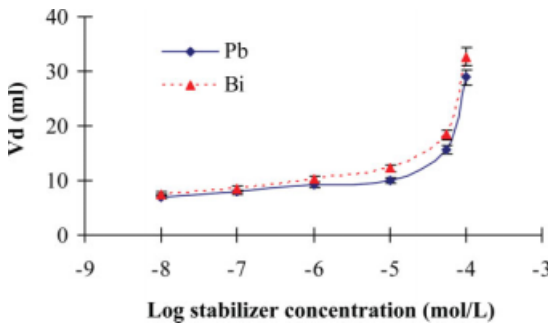

Figure 9. The dependence of decomposition volume (V_d) on the concentration of stabilizer used.

[Color figure can be viewed in the online issue, which is available at www.interscience.wiley.com.]

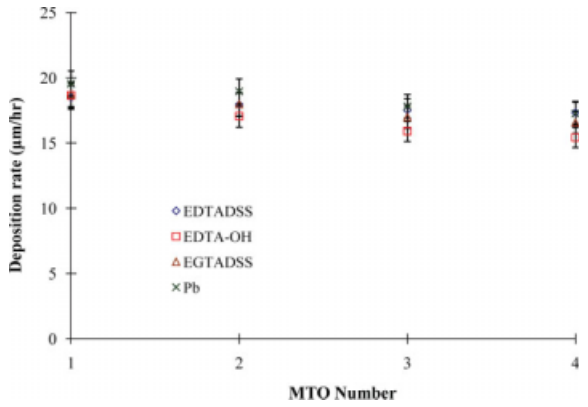

Figure 10. The change of nickel deposition rate with the increase in MTO in the plating bath containing different Bi^{3+}-complex ions and Pb^{2+} ion as reference.

[Color figure can be viewed in the online issue, which is available at www.interscience.wiley.com.]

Table 3. Change of the Ni and P Contents in the Plating Layer with MTO

Round of MTO	EDTADSS Ni wt.%	EDTADSS P wt.%	EDTA-OH Ni wt.%	EDTA-OH P wt.%	EGTADSS Ni wt.%	EGTADSS P wt.%
1	88.9	11.1	89.5	10.5	88.6	11.4
2	88.9	11.1	89.1	10.9	88.4	11.6
3	88.1	11.9	89.2	10.8	88.2	11.8
4	88.0	12.0	89.2	10.8	88.4	11.6

Evaluation of corrosion resistance) was used to study the chemical corrosion resistance of the plating layers obtained from different MTOs (Figure 11). It turns out that the corrosion potential (E_{corr}) shifts to negative direction with each MTO-cycle. Generally the anodic polarization curves observed can be divided into two regions (using M-1 curve as an example). The first region embraces potentials between E_{corr} and approximately −0.1 V (wrt. Ag/AgCl). This is the region where the dissolution of Ni-P deposit is kinetically limited. The anodic current density increases slowly with potential moving to more positive. The second region is at potentials above −0.1 V, where the transpassive dissolution of Ni/P alloys begins, and the anodic current density increases quickly with the potential of moving toward a positive direction.[33,34]

The overall results of the three ENP baths show that the anodic (corrosion) current density values increase with the extension of operation time regardless of the kind of EDTA derivative used in forming Bi^{3+}-complex ion stabilizer (Figure 12). As noted previously that the MTO does not bring about significant changes in the Ni/P ratio of plating layer, a rough surface morphology would be likely to be another factor reducing the corrosion resistance. The plating layers generated from the bath using Bi^{3+}-(EDTA-OH) complex ion as stabilizer are chosen as the demo samples (Figure 13). The

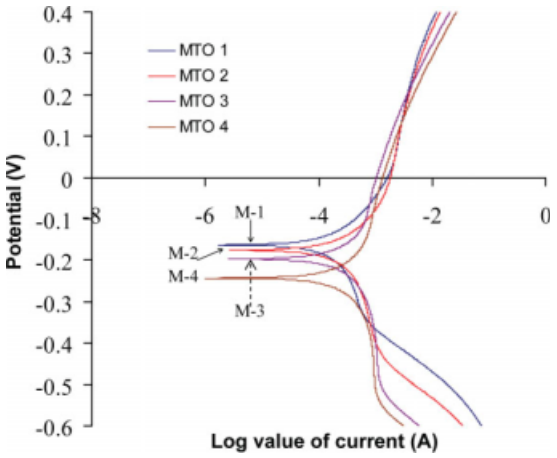

Figure 11. The PDS curves of the different Ni-P plating layers produced from different rounds of MTO in the same plating bath where the Bi^{3+}-EGTADSS complex (10^{-6}mol/L) was used as stabilizer.

[Color figure can be viewed in the online issue, which is available at www.interscience.wiley.com.]

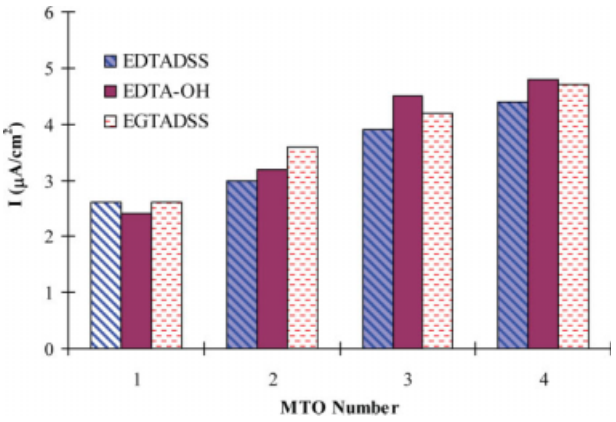

Figure 12. The corrosion current density on the Ni-P plating layer vs. MTO number, in which the effects of the three Bi^{3+} complexes are displayed.

[Color figure can be viewed in the online issue, which is available at www.interscience.wiley.com.]

first MTO produced the smoothest and cleanest surface among the four samples. It, thus, gave rise to the smallest corrosion current density. Nevertheless, the plating layers generated from the later MTO cycles showed some co-deposition of insoluble tiny particles on their surfaces, which is deemed to increase susceptibility to galvanic corrosion. We are, therefore, inclined toward the view[2] that this phenomenon is caused by the aging of plating solution, namely the accumulation of the plating byproducts in the solution through continuous operation. Hence, the reduction in corrosion resistance has little to do with the type and concentration of Bi^{3+}-complex ions. For comparison purpose, the micrograph of the surface of Ni-P layer, which was deposited in the solution with using Pb^{2+} ion stabilizer, was examined as well. There are a number of pinholes on it due to the dwelling of H_2 bubbles generated at the surface during plating.[35] It is considered that the use of Pb^{2+} ion stabilizer causes slow departing of H_2 bubbles from microscale rough surface as exhibited in the micrograph.

Conclusion

This work investigates a lead-free electroless nickel plating (ENP) bath in which three bismuth(III) complexes are tested, respectively, as the bath stabilizer. The EDTA derivatives — EDTADSS, EDTA-OH and EGTADSS — are found to be able to form soluble complexes with Bi^{3+} ion in the acidic ENP solutions. The relation of ENP deposition rate with concentration of stabilizer was investigated; all the three kinds of Bi^{3+}-complex ions cause a rapid decrease in the ENP rate at the critical concentration in the vicinity of 10^{-5} M. Below this critical concentration, bismuth complexes show minor effect on the ENP rate and the composition of Ni-P deposition layer. Furthermore, the anodic reaction of hypophosphite on a Ni-P electrode in the presence of one of the Bi^{3+}-complex ions is tested via measuring the anodic current density. The plots of current density vs. stabilizer concentration resulted from this test are analogous to

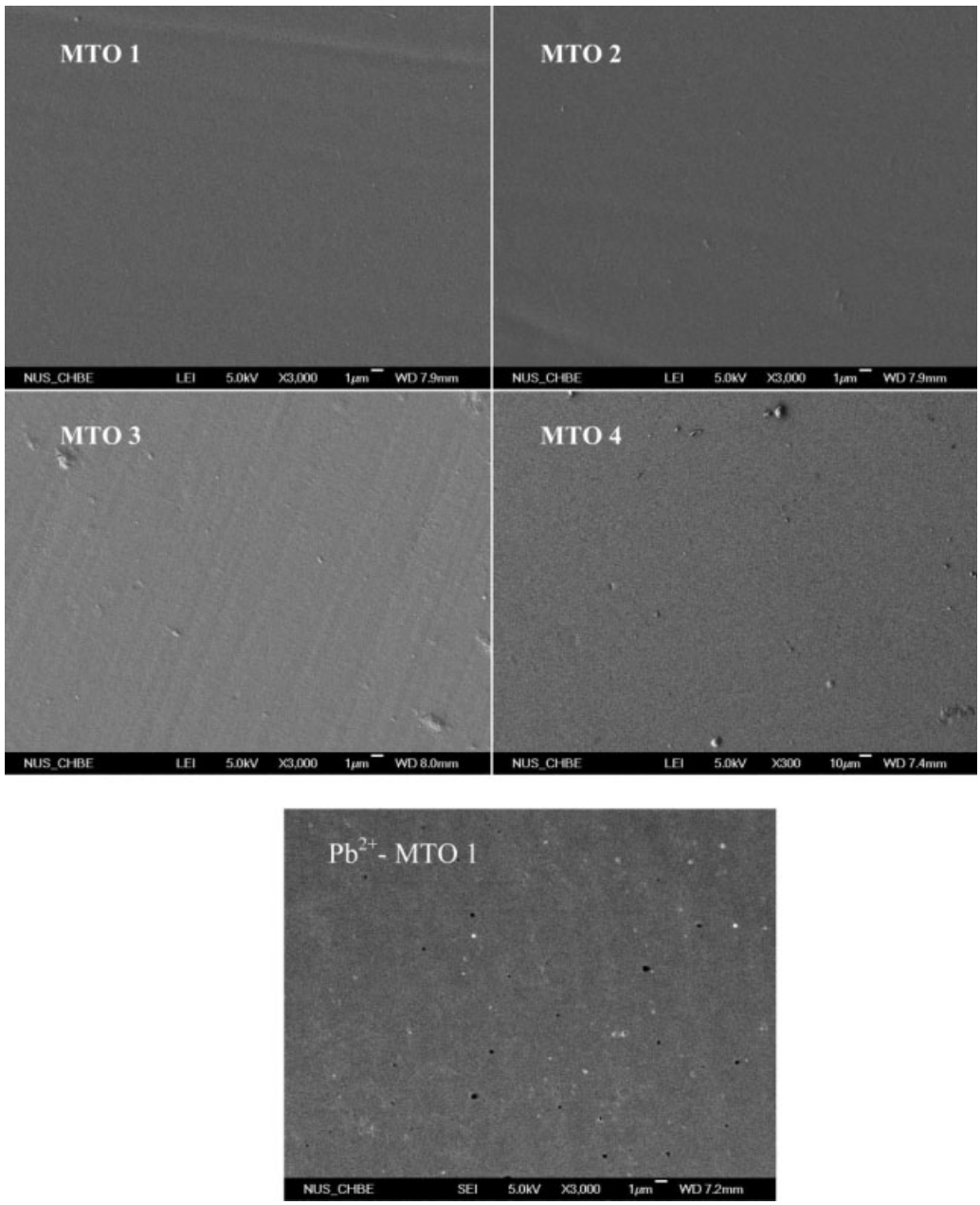

Figure 13. A demonstration of the surface morphology of the 4 MTO samples from the plating bath using the Bi^{3+}-(EDTA-OH) complex as the stabilizer.

those of the deposition rate vs. stabilizer concentration. According to the potentiostat test, EDX and XPS analyses, Bi^{3+}-complex ions are believed to undertake chemical displacement reaction with Ni(0) atoms, in which Bi(0) atoms are produced and then passivate the oxidation of hypophosphite ion at anode. Consequently, both nickel and phosphorus deposition rates are reduced due to electron deficiency. A modified kinetic model is established through successful simulation of the experimental curves of plating rate-stabilizer concentration relation. The last part of this work investigates the durability of the Bi^{3+}-complex ion in a 4-MTO continuous ENP process. As a key parameter, the electrochemical corrosion resistance of the resulting Ni-P deposition layers is assessed. The result shows that the corrosion resistance decreases with an extension of operation time due to the co-deposition of tiny particles.

Literature Cited

1. Riedel W. *Electroless Nickel Plating*. Stevenage, Herts.: ASM International Finishing Publications; 1991.
2. Mallory GO, Haydu JB, eds. *Electroless plating-fundamentals and applications*. Orlando: American Electroplaters and Surface Finishers Society; 1990.
3. Schlesinger M, Paunovic M, eds. *Modern electroplating*. 4th ed. New York: John Wiley & Sons, Inc.; 2000.
4. Sadeghi M, Longfield PD, Beer CF. Effects of heat treatment on the structure, corrosion resistance and stripping of electroless nickel coating. *Trans Inst Met Finish*. 1983;61:141–146.

5. Castellino N, Castellino P, Sannolo N, eds. *Inorganic Lead Exposure: Metabolism and Intoxication*. FL: Lewis Publishers; 1995.
6. Chen CH, Chen BH, Hong L. Role of Cu^{2+} as an additive in an electroless nickel-phosphorus plating system: A stabilizer or a codeposit? *Chem Mater*. 2006;18:2959–2968.
7. Cheong WJ, Luan BL, Shoesmith DW. Protective coating on Mg AZ91D alloy - The effect of electroless nickel (EN) bath stabilizers on corrosion behaviour of Ni-P deposit. *Corr Sci*. 2007;49:1777–1798.
8. Cheong WJ, Luan BL, McIntyre NS, Shoesmith DW. XPS characterization of the corrosion film formed on the electroless nickel deposit prepared using different stabilizers in NaCl solution. *Surf Interface Anal*. 2007;39:405–414.
9. Lin KL, Hwang JW. Effect of thiourea and lead acetate on the deposition of electroless nickel. *Mater Chem Phys*. 2002;76:204–211.
10. Das L, Chin DT. Effect of bath stabilizers on electroless nickel deposition on ferrous substrates. *Plat Surf Finish*. 1996;83:55–61.
11. Cheong WJ, Luan BL, Shoesmith DW. The effects of stabilizers on the bath stability of electroless Ni deposition and the deposit. *Appl Surf Sci*. 2004;229:282–300.
12. Han KP, Jing LF. Stabilization effict of electroless nickel plating by thiourea. *Met Finish*. 1997;5:73–75.
13. Zylberberg J, Belik AA, Takayama-Muromachi E, Ye ZG. Bismuth aluminate: A new high-T-c lead-free piezo-/ferroelectric. *Chem Mater*. 2007;19:6385–6390.
14. Ketkar SA, Umarji GG, Phatak GJ, Ambekar JD, Rao IC, Mulik UP, Amalnerkar DP. Lead-free photoimageable silver conductor paste formulation for high density electronic packaging. *Mater Sci Eng B*. 2006;132:215–221.
15. Sano Y, Satoh H, Chiba M, Shinohara A, Okamoto M, Serizawa K, Nakashima H, Omae K. Oral toxicity of bismuth in rat: Single and 28-day repeated administration studies. *J Occup Health*. 2005;47:293–298.
16. Sano Y, Satoh H, Chiba M, Shinohara A, Okamoto M, Serizawa K, Nakashima H, Omae K. A 13-week toxicity study of bismuth in rats by intratracheal intermittent administration. *J Occup Health*. 2005;47:242–248.
17. Serfontein WJ, Mekel R, Bank S, Barbezat G, Novis B. Bismuth toxicity in man - I. Bismuth blood and urine levels in patients after administration of a bismuth protein complex (Bicitropeptide). *Res Commun Chem Pathol Pharmacol*. 1979;26:383–839.
18. Alfons H, Heinz-Peter B. Lead-free Chemical Nickel Alloy. *US2004007472*; 2004:01–15.
19. Bobrovskaya VP, Sokolov VG, Yurkevich VV. Effect of Bi(III) on electroless nickel plating. *Vestn Beloruss Gos Univ*. 1993;2:16–18.
20. Yin X, Hong L, Chen BH. Role of a Pb^{+} stabilizer in the electroless nickel plating system: A theoretical exploration. *J Phys Chem B*. 2004;108:10919–10929.
21. Yin X, Hong L, Chen BH, Ko TM. Modeling the stability of electroless plating bath - diffusion of nickel colloidal particles from the plating frontier. *J Colloid Interface Sci*. 2003;262:89–96.
22. Izumi O, Osamu W, Shiro H. Anodic oxidation of reductants in electroless plating. *J Electrochem Soc*. 1985;132:2323–2330.
23. Gyanutene I, Lyankaitene Y. The effect of nitrogen-containing organic compounds on the autocatalyzed hypophosphite reduction of nickel(II). *Zashchita Metallov*. 1996;32:593–597.
24. Khaldeev GV, Petukhov IV, Shcherban MG. Electrooxidation of the hypophosphite ion on a palladium electrode. *Elektrokhimiya*. 2000;36:934–941.
25. Sotskaya NV, Goncharova LG, Kravchenko TA, Zhivotova EV. Effect of phosphite ions on the kinetics of nickel deposition by hypophosphite. *Elektrokhimiya*. 1997;33:485–489.
26. Han KP, Jing LF. Stabilization effict of electroless nickel plating by thiourea. *Met Finish*. 1997;5:73–75.
27. Ohno I, Wakabayashi O, Haruyama S. Anodic oxidation of reductants in electroless plating. *J. Electrochem. Soc*. 1985;132:2323–2330.
28. Lyaukonis YY, Yusis ZZ. *Issledovaniya voblasti osazhdeniya metallov. vol.9 (Studies in the Metal Deposition Field)*. Vilnius: Institute of Chemistry and Chemical Technology, Lithuanian Academy of Sciences; 1983.
29. Moulder JF, Stickle WF, Sobol PE, Bomben KD.*Handbook of X-ray Photoelectron Spectroscopy*.Boston:Perkin-Elmer Cooperation Physical Electronics Division; 1992.
30. Suezer S, Ertase N, Ataman OY. XPS Characterization of Bi and Mn collected on atom-trapping silica for AAS. *Applied Spectroscopy*. 1999;53:479–482.
31. Carbajal JL, White RE. Electrochemical production and corrosion testing of amorphous Ni-P. *J Electrochem Soc*. 1988;135:2952–2956.
32. Luke DA. Nickel phosphorus electrodeposits. *Trans Inst Met Finish*. 1986;64:99–104.
33. Lo PH, Tasi WT, Lee JT, Hung MP. Role of phosphorus in the electrochemical behavior of electroless Ni-P alloys in 3.5 wt % NaCl solutions. *Surf Coat Technol*. 1994;67:27–34.
34. Ashassi-Sorkhabi H, Rafizadeh SH. Effect of coating time and heat treatment on structure and corrosion characteristics of electroless Ni-P alloy deposits. *Surf Coat Technol*. 2004;176:318–326.
35. Chen BH, Hong L, Ma Y, Ko TM. Effects of surfactants in an electroless nickel-plating bath on the properties of Ni-P alloy deposits. *Ind Eng Chem Res*. 2002;41:2668–2678.

Manuscript received May 16, 2008, and revision received Nov. 25, 2008.